Improved scattering analysis of arbitrary-shaped cylinders in a focused beam system using Gabor representation

R.Shavit

Abstract: Gabor expansion is used to reconstruct the scattering pattern and the induced field ratio (IFR) of an arbitrarily-shaped cylinder measured in a focused beam system. The fields of the transmitting and receiving antennas in the measurement system are described by equivalent fundamental Gaussian beams. The results obtained by the proposed method of analysis verify well with the scattering characteristics computed analytically or numerically by the method of moments (MoM), finite elements method (FEM) and by a previous method of analysis using an FFT algorithm.

1 Introduction

The ability to compute and measure the scattering characteristics of an arbitrary-shaped cylinder is essential to the entire scattering analysis of large sandwich and metal space frame radomes. The scattering characteristics of an arbitrary-shaped cylinder is characterised by its forward scattering value (IFR) and its scattering pattern. The concept of IFR was introduced by Kay [1] for modelling metal space frame radomes. Both IFR and scattering pattern are defined for uniform plane wave illumination. Some deficiencies in the IFR approach have been discussed in [2], and a more rigorous approach based on the full 2×2 scattering matrix from an individual beam/seam was proposed by [3, 4].

Analytical and numerical computations of the scattering characteristics from cylinders can be performed, but in many cases these techniques are quite laborious and time consuming. Consequently, in many practical instances to speed up the developing process, control manufacturing process and verify the numerical computation, an accurate measurement technique of the IFR and the scattering pattern is required. Few experimental procedures [5, 6] were proposed to determine the scattering characteristics. However, these methods either lack the capability to measure the scattering pattern [5] or lack the capability to filter out reflections from surrounding objects [6]. In a previous paper [7], a new combined experimental and numerical procedure based on a focused beam system was proposed. The unique feature of the focused beam system is its capability to filter out specular and diffuse reflections from adjacent objects. The Gaussian-type characteristics of the transmitting and receiving beams in such a system avoids direct measurement of the IFR and the scattering pattern for uniform plane wave illumination and a reconstruction procedure to compensate for the perturbation caused by the Gaussian illumination of the cylinder is necessary. A correction algorithm, based on FFT, was proposed to reconstruct the scattering characteristics of the cylinder.

The current paper describes an improved and more efficient algorithm to reconstruct the scattering characteristics of a cylinder, based on measurements taken in a focused beam system. In the proposed procedure, the scattered field is expanded in terms of Gabor series functions [8] and the data is manipulated to reconstruct the scattering pattern and the IFR for uniform plane wave illumination.

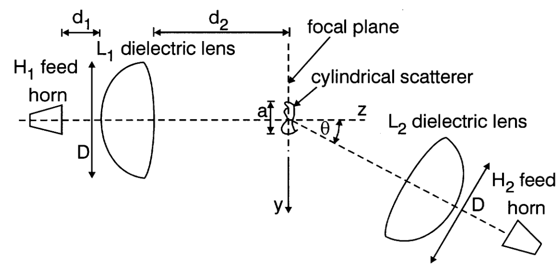

Fig. 1 *Schematic configuration of focused beam system*

2 Method description

The schematic configuration of the measurement system is shown in Fig. 1. The system is composed of two circular identical dielectric lenses L_1 and L_2 with diameter D and two feed horns H_1 and H_2 with aperture dimensions $A * B$ and linear polarisation. Each lens is designed to have two focal points located at distances f_1 and f_2 from the opposite sides of the lens surface. The actual distance of the feed horn phase centre from the lens surface is d_1. In principle, it is desired that $f_1 = d_1$; however, due to the movement of the feed horn phase centre with frequency this requirement is not perfectly achieved. The energy radiated by H_1 feed horn is captured by L_1 lens, focused on the opposite side to the common focal point of the two lenses at a distance d_2 from the lens surface, radiated into the L_2 lens and focused again into the receiving H_2 feed horn. We define the focal plane ($z = 0$) of the system as the plane passing through the internal (common) focal point of the two lenses and perpendicular to the system axis. In the measurement to be

IEE Proceedings online no. 19990340

DOI: 10.1049/ip-map:19990340

Paper first received 19th October 1998 and in revised form 23rd February 1999

The author is with the Department of Electrical and Computer Engineering, Ben-Gurion University of the Negev, Beer Sheva 84105, Israel

described, the cylindrical scatterer will be located in this focal plane on the system axis.

In this paper, we made the assumption that the propagation mechanism of the focused beam system can be described by an inward and an outward Gaussian beam with common waists in the focal plane (z = 0). The minimum waists in the focal plane are w_{0x} and w_{0y} representing the field distribution in x and y directions, respectively. The received signal is set to zero (amplitude and phase) before the cylinder is moved into the focal plane. In the next step, the cylinder is brought into the focal plane on the system axis and the relative amplitude $\Delta\alpha$ and phase $\Delta\phi$ of the received signal $R(y) = \Delta\alpha e^{j\Delta\phi}$ is recorded. Then the receiving lens is rotated in predetermined angular increments on an arch with its centre of rotation located on the system axis in the focal plane. For each angular point, two readings are taken with and without the cylinder.

The angular dependence of the transmission loss between the two feed horns is proportional to the coupling between the inward and outward Gaussian beams in the focal plane. In the case where the scatterer is absent, it has been shown [7] that this coupling factor $C_c(\theta)$ is equal to:

$$C_c(\theta) = C_0 e^{-\frac{1}{2}\left(\frac{w_{0y}\pi}{\lambda}\sin(\theta)\right)^2} \tag{1}$$

in which C_0 is the coupling coefficient between the two beams, when the two lenses are aligned (θ = 0). The coupling factor $C_c(\theta)$ can be either computed through eqn. 1 or directly measured.

2.1 System analysis with the cylindrical scatterer

In this case, the signal received by H_2 feed horn is proportional to the coupling $C_t(\theta)$ between the outward Gaussian beam represented by the field distribution $f_r(x, y)$ and the total electric field in the vicinity of the cylinder (z = 0). Thus, $C_t(\theta)$ can be expressed as shown in [9] by:

$$C_t(\theta) = \int_{-\infty}^{\infty}\int_{-\infty}^{\infty} (f_t + f_{sq}) f_r^* \, dx\, dy \tag{2}$$

where $f_t(x, y)$ is the inward Gaussian beam distribution and $f_{sq}(x, y)$ is the scattered electric field by the cylinder in the focal plane. In a focused beam system, $f_{sq}(x, y)$ can be approximated [7] by:

$$f_{sq}(x,y) = \begin{cases} f_s(y) e^{-\frac{x^2}{w_{0x}^2} - \frac{y^2}{w_{0y}^2}} & |y| \le \frac{a}{2}, |x| < \infty \\ 0 & \text{elsewhere} \end{cases} \tag{3}$$

where $f_s(y)$ is the scattered field distribution from the cylinder in the focal plane for uniform plane wave illumination and a is the projected width of the cylinder on the focal plane. If we denote by $C_s(\theta)$ the coupling between the scattered field by the cylinder $f_{sq}(x, y)$ and the field of the non-aligned outward Gaussian beam $f_r(x, y)$, it has been shown in [7] that:

$$\begin{aligned} C_s(\theta) &= C_t(\theta) - C_c(\theta) \\ &= \int_{-\infty}^{\infty}\int_{-\infty}^{\infty} f_{sq} f_r^* \, dx\, dy \\ &= C_{s0} \int_{-a/2}^{a/2} f_{sp}(y) e^{jky\sin\theta} dy \end{aligned} \tag{4}$$

in which, $C_{so} = (2/\pi w_{oy}{}^2)^{1/2}$ is a normalisation factor and $f_{sp}(y) = f_s(y)e^{-2(y/w_{oy})^2}$. One can observe that $C_s(\theta)$ has the form of the far field radiation pattern [10] of an equivalent aperture distribution $f_{sp}(y)$ located in the focal plane, while our interest is in the radiation pattern of the field distribution $f_s(y)$ excited by a uniform plane wave illumination.

In a focused beam system, it will be natural to expand the equivalent aperture distribution $f_{sp}(y)$ in terms of functions with Gaussian characteristics, like the Gabor series functions with Gaussian distribution [8]. If we follow the procedure outlined in [11], $f_{sp}(y)$ can be rewritten in the form:

$$f_{sp}(y) = \sum_m \sum_n A_{mn} g(y - mL) e^{-jn\Omega y}$$
$$\Omega \cdot L = 2\pi \tag{5}$$

in which $g(y)$ are the normalised Gabor functions with Gaussian distribution:

$$g(y) = \left(\frac{2^{1/2}}{L}\right)^{1/2} e^{-\pi\left(\frac{y}{L}\right)^2} \tag{6}$$

and A_{mn} are the unknown coefficients of these functions. One can observe that the Gabor representation expands the function $f_{sp}(y)$ in terms of displaced and inclined Gaussian functions. The free parameters L and Ω are determined by convergence tests of eqn. 5. Criteria for the particular choice of L are discussed in [11]. If we denote $\eta = k\sin\theta$ and substitute eqn. 5 into eqn. 4, we obtain after performing the analytical integration that:

$$C_s(\eta) = C_{s0} \sum_m \sum_n A_{mn} G(\eta - n\Omega) e^{jmL\eta} \tag{7}$$

where

$$G(\eta) = \left(\frac{2^{3/2}\pi}{\Omega}\right)^{1/2} e^{-\pi\left(\frac{\eta}{\Omega}\right)^2} \tag{8}$$

is the Fourier transform of $g(y)$. In the actual measurement, we normalise the received signal at each angle to C_0, the value recorded at θ = 0 without the scatterer, and we can compute $C_s(\eta)$ based on eqn. 4. Thus, the only unknown quantity in eqn. 7 are the coefficients A_{mn}. The coefficients A_{mn} in eqn. 7 may be evaluated with the aid of the so-called biorthogonal function $\gamma(y)$ defined implicitly [12] by:

$$\int_{-\infty}^{\infty} g(y)\gamma^*(y - mL) e^{jn\Omega y} dy = \delta_m \delta_n$$
$$\delta_m = \begin{cases} 1 & m = 0 \\ 0 & m \ne 0 \end{cases} \tag{9}$$

In [12] it has been shown that the explicit form of $\gamma(y)$ is:

$$\gamma(y) = \left(\frac{\pi^3}{2^{1/2} L K_0^3}\right)^{1/2} e^{\pi\left(\frac{y}{L}\right)^2} \sum_{n \ge \frac{y}{L} - \frac{1}{2}} (-1)^n e^{-\pi\left(n + \frac{1}{2}\right)^2} \tag{10}$$

in which K_0 = 1.85407468. If we denote by $\Gamma(\eta)$ the Fourier transform of $\gamma(y)$, multiply both sides of eqn. 7 by $(1/2\pi)\Gamma^*(\eta - n\Omega)e^{-jmL\eta}$, integrate over the interval $[-\infty, \infty]$ and implement the biorthogonal relation (eqn. 9), we obtain:

$$A_{mn} = \frac{1}{2\pi C_{s0}} \int_{-\infty}^{\infty} C_s(\eta)\Gamma^*(\eta - n\Omega) e^{-jmL\eta} d\eta \tag{11}$$

Alternatively, if we express $\Gamma(\eta)$ in terms of $\gamma(y)$ and observe that $C_s(\eta)$ is the Fourier transform of $f_{sp}(y)$, eqn. 11 can be rewritten in the form:

$$A_{mn} = \frac{1}{C_{s0}} \int_{-a/2}^{a/2} f_{sp}(y)\gamma^*(y+mL)e^{-jn\Omega y}dy \quad (12)$$

Eqn. 11 enables us to compute the coefficients A_{mn} as a function of $C_s(\eta)$. The function $f_{sp}(y)$ is band limited in the interval $[-a/2, a/2]$; therefore using the sampling theorem $C_s(\eta)$ can be expressed by:

$$C_s(\eta) = \sum_l C_s(l\eta_0)\frac{\sin(\eta - l\eta_0)a/2}{(\eta - l\eta_0)a/2} \qquad \eta_0 = \frac{2\pi}{a} \quad (13)$$

A simplification to the above can be obtained if we recognise that $C_s(\eta)$ is band limited in the visible range $[-k, k]$. In this case, we may truncate the summation with the upper bound being approximated by $L_p \approx a/\lambda$. Substitution of eqn. 13 into eqn. 11 and performance of the analytical integration yields,

$$A_{mn} = \frac{1}{C_{s0}a} \sum_{l=-L_p}^{L_p} C_s(l\eta_0) \times \int_{-a/2}^{a/2} \gamma^*(y+mL)e^{-j(n\Omega - l\eta_0)y}dy \quad (14)$$

Once the coefficients A_{mn} are computed, either by using eqn. 11 or eqn. 14, one can compute $f_{sp}(y)$ using eqn. 5 and consequently $f_s(y)$ the scattered field distribution from the cylinder in the focal plane for uniform plane wave illumination using the relation:

$$f_s(y) = f_{sp}(y)e^{2\left(\frac{y}{w_{0y}}\right)^2} \text{ in the range } [-a/2, a/2]$$

If we follow the procedure outlined in [7], knowledge of $f_s(y)$ enables us to compute the scattering radiation pattern $E_s(\theta)$ for uniform plane wave illumination using [10]:

$$E_s(\theta) = \int_{-a/2}^{a/2} f_s(y)e^{jk\sin\theta y}dy \quad (15)$$

Alternatively, knowledge of $f_s(y)$ enables us to compute a new set of coefficients A_{mn} using eqn. 12 and the reconstructed scattering radiation pattern using eqn. 7. Moreover, the IFR can be computed using [7]:

$$IFR = \left(10^{\frac{\Delta\alpha}{20}}e^{j\Delta\phi} - 1\right)\sqrt{\frac{\pi}{2}}\frac{w_{0y}}{a}\frac{\int_{-a/2}^{a/2} f_s(y)dy}{\int_{-a/2}^{a/2} f_s(y)e^{-\frac{2y^2}{w_{0y}^2}}dy} \quad (16)$$

in which $\Delta\alpha$(dB) denote the change in amplitude and $\Delta\phi$ the change in phase, when the cylinder is brought to the focal plane on the system axis.

3 Numerical results

In [7] it was reported about a focused beam system built to validate the theoretical approach using an FFT algorithm. Two AEL antenna horns model H-1498 operating in the frequency range 2–18GHz were chosen as feeds with almost constant 10dB beamwidth in both E and H planes over the entire frequency bandwidth. The diameter of the lens was chosen to be 55.9cm, and it was manufactured from material with dielectric constant 2.3. The lens focal distances f_1 and f_2 were chosen as 53.3cm and 203.2cm, respectively. At the operating frequency 12GHz, the Gaussian beam waist size w_{0x} and w_{0y} in the focal plane were measured to be 6.45cm and 6.78cm, respectively, at –8.7dB points (the field is e^{-1} of its value on axis).

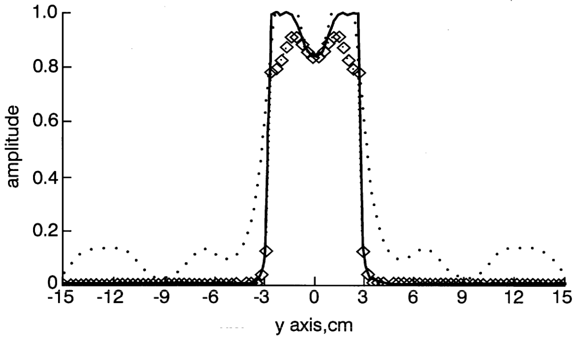

Fig. 2 *Electric field distribution $f_{sp}(y)$ of dielectric beam 1.2 × 5.71cm in focal plane of focused beam system compared to field distribution for uniform plane wave illumination at 12GHz (vertical polarisation) using FFT and Gabor algorithms*
····◇···· $f_{sp}(y)$
——— $f_s(y)$ with Gabor
·········· $f_s(y)$ with FFT

Two rectangular cylinders (metal and dielectric) used in a typical metal and dielectric space frame radomes were chosen for the theoretical verification. The cross-section of the metal beam was 1.37 × 5.16cm and that of the plastic beam was 1.2 × 5.71cm with ε_r = 5.0. The cylinders were tested at 12GHz for both vertical (VP) and horizontal (HP) polarisations and for two incident angles (broadside and narrow side). One can observe that, in our case, the projected cylinder width a vary between 0.48λ to 2.28λ. Due to physical constraints of the measurement setup, the angular extent of our focused beam was θ_{max} = 70°. The limitation posed on $C_s(\eta)$ to be band limited in the visible range limits the algorithm to apertures $a > \lambda$. In cases where $a < \lambda$ the perturbation due to the Gaussian illumination of the cylinder is negligible and the scattering radiation pattern is directly proportional to the measurement of $C_s(\eta)$ as discussed in [7]. The beams were illuminated on their broadside ($a > \lambda$). Consequently, the number of angular measurements in the visible range $[-k\sin\theta_{max}, k\sin\theta_{max}]$ is equal to 5. Moreover, due to the symmetry of the scattering radiation pattern, it will be sufficient to use only about half of this quantity. For comparison, the FFT algorithm detailed in [7] required more than ten times more angular measurements to reproduce the scattering radiation pattern. The choice of the Gaussian parameter L affects the truncation properties of the summation in eqns. 5 and 7. As discussed in [11] the minimum number of elements in these summations is obtained, if we make the choice $L \simeq a/2$. For this choice the upper bound M of the index m is $|m| < M \simeq a/2L$ and the upper bound of the index n is $|n| \leq N \simeq k/\Omega = L/\lambda$. The recorded data was processed with an FFT algorithm as described in [7] and using Gabor series representation to evaluate the field distribution of the scatterer $f_s(y)$ in the focal plane. In the FFT algorithm, we used 27 angular measurements and performed interpolation to obtain 2048 points. Fig. 2 shows the field distribution $f_s(y)$ computed with the Gabor series representation compared with that computed with the FFT algorithm and to the perturbed field distribution $f_{sp}(y)$ for the dielectric beam illuminated on its broadside and for vertical polarisation. One can observe a relatively good agreement between the results obtained with the two algorithms, considering the fact that using the Gabor representation only three angular data

Table 1: Comparison between measured and computed IFR values

	Vertical polarisation						Horizontal polarisation					
	IFR amplitude			*IFR* phase (deg.)			*IFR* amplitude			*IFR* phase (deg.)		
Cylinder type	MoM/ FEM	using FFT reconst. algor.	using Gabor reconst. algor.	MoM/ FEM	using FFT reconst. algor.	using Gabor reconst. algor.	MoM/ FEM	using FFT reconst. algor.	using Gabor reconst. algor.	MoM/ FEM	using FFT reconst. algor.	using Gabor reconst. algor.
Plastic $a = 5.71$cm	1.91	1.93	1.93	158.8	162.4	162.9	1.79	1.84	1.83	162.6	164.0	166.5
Metal $a = 5.16$cm	1.14	1.20	1.11	172.6	171.6	172.9	0.98	1.0	1.1	–176.6	177.2	179.3

measurements points were used. Fig. 3 shows the comparison among the computed scattering pattern by FEM [13], the reconstructed scattering pattern using the Gabor representation using $M = 5$, $N = 7$, $L_p = 2$ and the reconstructed pattern using the FFT algorithm. Again, one can observe a relatively good agreement in the main beam and in the sidelobe level, when we compare the computed and the reconstructed pattern. The difference in the sidelobe level width may be caused by insufficient compliance with the requirement posed on $C_s(\eta)$ to be a band limited function. The ripple in the reconstructed pattern at $\theta \simeq 12°$ and 23° is probably caused by inaccurate angular position readings.

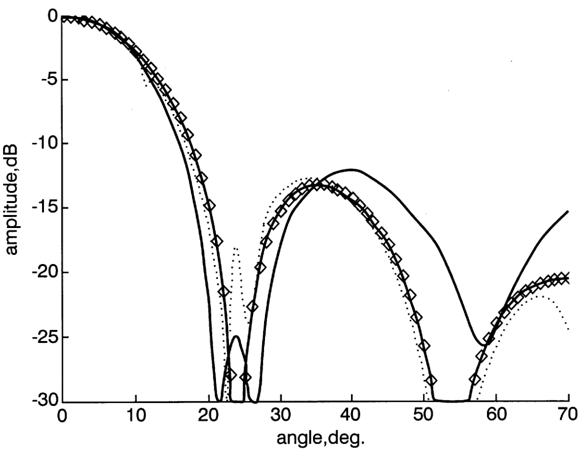

Fig. 3 *Comparison among computed and reconstructed scattering radiation patterns of dielectric beam 1.2 × 5.71cm illuminated on its broadside at 12GHz (vertical polarisation) using FFT and Gabor algorithms*
——— reconst. w/Gabor
.... reconst. w/FFT
—◇— computed (FEM)

The data from all measurements taken for both the plastic and metal beams were processed to obtain the IFR based on eqn. 16. The results obtained were compared to the IFR values computed numerically by two existing codes developed by the University of Illinois, Urbana, IL, USA. One is a FEM code [13] for dielectric beam scattering analysis and the other is a MoM code [14] for metallic beam scattering analysis. Computation results of the IFR for the various types of cylinders by the three methods at 12 GHz are shown in Table 1.

One can observe a good agreement between the numerical computation (MoM and FEM) and the computed values using both reconstructing algorithms FFT and Gabor representation.

4 Summary

An improved numerical procedure based on Gabor series representation of the scattered field in front of a cylinder positioned in a focused beam system was used to reconstruct the scattering radiation pattern for plane wave illumination. The analysis was based on the assumption that the electric fields between the lenses can be described by fundamental Gaussian beams. The analysis gives good results if the projected aperture in the focal plane, satisfies the condition $a > \lambda$. The algorithm reduces significantly the required angular data measurements to reconstruct the scattering radiation pattern in comparison to a previous procedure [7] based on an FFT algorithm. The information obtained on the scattering pattern helps to refine the calculations of the scattering analysis for large space frame radomes.

5 Acknowledgments

The author thanks A. Mantz and C. Slotta for performing the measurements and T. Wells, A. Cohen, T. Monk and J. Sangiolo for very helpful and fruitful discussions. All are associated with ESSCO, Concord, MA, USA.

6 References

1 KAY, A.F.: ‘Electrical design of metal space-frame radomes’, *IEEE Trans.*, 1965, AP–13, pp. 188–202
2 ROBINSON, A.J., BENNETT, J.C., SMITH, F.C., and CHAMBERS, B.: ‘Evaluation of the EM performance of large ground based radomes’. Proceedings of the sixth *Electromagnetic structures* conference, Frierichshafen, Germany, 1991, pp. 121–124
3 JOY, E.B., EPPLE, M.B., and PUNNETT, M.B.: ‘Analysis of MSF radome using plane wave spectra techniques’. Proceedings of the joint third international conference on *Electromagnetics in aerospace applications* and the seventh European *Electromagnetic structures* conference, Torino, Italy, 1993, pp. 181–184
4 ROBINSON, A.J., CHAMBERS, B., and BENNETT, J.C.: ‘Technique for predicting the electromagnetic performance of impedance-loaded dielectric space-frame radome components’, *IEE Proc., Radar Sonar Navig.*, 1997, 144, (1), pp. 1–8
5 RUSCH, W.V.T., HANSEN, J.A., KLEIN, C.A., and MITTRA, R.: ‘Forward scattering from square cylinders in the resonance region with application to aperture blockage’, *IEEE Trans.*, 1976, AP–24, pp. 182–189
6 SHAVIT, R., COHEN, A., and NGAI, E.C.: ‘Characterization of the scattering parameters from arbitrary shaped cylinders by near-field probing’, *IEEE Trans.*, 1995, AP–43, pp. 1–5
7 SHAVIT, R., WELLS, T., and COHEN, A.: ‘Scattering analysis of arbitrarily shaped cylinders in a focused beam system’, *IEE Proc., Microw. Antennas Propag.*, 1998, 145, (4), pp. 284–289
8 GABOR, D.: ‘Theory of communication’, *J. Inst. Elec. Eng. (London)*, 1946, 93, (III), pp. 429–457
9 GOLDSMITH, P.F.: ‘Infrared and millimeter waves’ (Academic Press, New York, 1982)
10 ELLIOTT, R.S.: ‘Antenna theory and design’ (Prentice-Hall, New Jersey, 1981)
11 EINZIGER, P.D., RAZ, S., and SHAPIRA, M.: ‘Gabor representation and aperture theory’, *J. Opt. Soc. Am. A*, 1986, 3, (4), pp. 508–522
12 BASTIAANS, M.J.: ‘The expansion of an optical signal into a discrete set of Gaussian beams’, *Optik*, 1980, 57, pp. 95–101
13 MAHADEVAN, K., IRVINE, B., PEKEL, Ü., and MITTRA, R.: ‘Edge-based finite element analysis of singly and doubly periodic scatterers using absorbing and periodic boundary conditions’, *IEEE AP-S Int. Symp. Digest*, 1994, pp. 2136–2139
14 PETERSON, A.F., and KLOCK, P.W.: ‘An improved MFIE formulation for TE-wave scattering from lossy, inhomogeneous dielectric cylinders’, *IEEE Trans.*, 1988, AP–36, pp. 45–49